

## New High-Throughput Screening Assay To Reveal Similarities and Differences in Inhibitory Sensitivities of Multidrug ATP-Binding Cassette Transporters<sup>∇</sup>

Marcin Kolaczowski,<sup>1\*</sup> Anna Kolaczowska,<sup>2</sup> Noboru Motohashi,<sup>3</sup> and Krystyna Michalak<sup>1</sup>

Department of Biophysics, Wrocław Medical University, Ul. Chalubinskiego 10, 50-368 Wrocław, Poland<sup>1</sup>; Faculty of Veterinary Medicine, Wrocław University of Environmental and Life Sciences, Ul. Norwida 31, 50-375 Wrocław, Poland<sup>2</sup>; and Meiji Pharmaceutical University, 2-522-1 Noshio, Tokyo 2048588, Japan<sup>3</sup>

Received 18 July 2008/Returned for modification 23 October 2008/Accepted 18 January 2009

**Cdr1p is the major ATP-binding cassette multidrug transporter conferring resistance to azoles and other antifungals in *Candida albicans*. In this study, the identification of new Cdr1p inhibitors by use of a newly developed high-throughput fluorescence-based assay is reported. The assay also allowed monitoring of the activity and inhibition of the related transporters Pdr5p and Snq2p of *Saccharomyces cerevisiae*, which made it possible to compare its performance with those of previously established procedures. A high sensitivity, resulting from a wide dynamic range, was achieved upon high-level expression of the Cdr1p, Pdr5p, and Snq2p transporters in an *S. cerevisiae* strain in which the endogenous interfering activities were further reduced by genetic manipulation. An analysis of a set of therapeutically used and newly synthesized phenothiazine derivatives revealed different pharmacological profiles for Cdr1p, Pdr5p, and Snq2p. All transporters showed similar sensitivities to M961 inhibition. In contrast, Cdr1p was less sensitive to inhibition by fluphenazine, whereas phenothiazine selectively inhibited Snq2p. The inhibition potencies measured by the new assay reflected the ability of the compounds to potentiate the antifungal effect of ketoconazole (KTC), which was detoxified by the overproduced transporters. They also correlated with the 50% inhibitory concentration for inhibition of Pdr5p-mediated transport of rhodamine 6G in isolated plasma membranes. The most active derivative, M961, potentiated the activity of KTC against an azole-resistant *CDR1*-overexpressing *C. albicans* isolate.**

*Candida* yeasts are the fourth most common pathogens responsible for systemic bloodstream infections. *Candida albicans* is the most frequently isolated species, contributing to >50% of cases (41). It generally shows little permeability to a large variety of toxic compounds, which is believed to result to a large degree from the existence of an active permeability barrier (42). Cdr1p and Cdr2p are two homologous ATP-binding cassette (ABC) multidrug resistance (MDR) transporters of broad specificity that confer resistance to the most widely used azole antifungals as well as to terbinafine, amorolfine, and many other metabolic inhibitors (43, 48). *CDR1* is constitutively expressed in azole-sensitive isolates, where it modifies the intrinsic level of susceptibility to antifungals, as its inactivation by deletion increases sensitivity (47). The effectiveness of the small number of antifungals available for the treatment of life-threatening systemic mycoses is further reduced by overexpression of both *CDR1* and *CDR2* in many azole-resistant clinical isolates (46, 59).

Cdr1p and Cdr2p are structural and functional homologues of the Pdr5p and Snq2p MDR transporters of the model yeast *Saccharomyces cerevisiae* (25, 29, 50). A large-scale screening of Pdr5p substrate specificity identified it as the most important MDR ABC transporter, conferring resistance to most

classes of currently available antifungals and other xenobiotics, with some overlap in specificity with Snq2p and Yor1p (25). Pdr5p, Snq2p, and Yor1p become highly overproduced in the plasma membrane as a result of gain-of-function point mutations in the homologous Zn<sub>2</sub>Cys<sub>6</sub> transcriptional activators Pdr1p and Pdr3p, which can readily be selected on drug-containing media (1, 6, 7, 8, 22).

The development of efflux pump inhibitors for combination therapeutic approaches aimed at circumventing resistance is one strategy to increase the efficiency of currently available antifungals. Despite the identification of a few compounds reversing yeast azole resistance, including peptide derivatives and unnarmicins, by means of conventional, growth-based screening (39, 54), progress in the isolation and detailed quantitative characterization of new efflux pump inhibitors is limited by the lack of convenient and fast screening assays. In this study, taking advantage of high-level expression of Cdr1p and the closely related transporters Pdr5p and Snq2p in the model nonpathogenic yeast *S. cerevisiae*, we developed a new cell-based high-throughput assay for MDR transporter inhibition. The assay allowed the identification and characterization of new Cdr1p inhibitors and revealed differences in sensitivity of the three transporters that correlated with results obtained using previously established procedures based on cell growth and transport measurements in plasma membrane fractions (27). The effect of the most active inhibitor on the modulation of ketoconazole (KTC) resistance of a *CDR1*-overexpressing *C. albicans* isolate was also verified.

\* Corresponding author. Mailing address: Department of Biophysics, Wrocław Medical University, Ul. Chalubinskiego 10, 50-368 Wrocław, Poland. Phone: (48) 71 7841403. Fax: (48) 71 7840088. E-mail: mkolacz2@poczta.onet.pl.

<sup>∇</sup> Published ahead of print on 2 February 2009.

## MATERIALS AND METHODS

**Reagents.** The following reagents were purchased from the indicated suppliers: yeast extract, tryptone, peptone, and agar, Becton Dickinson; glucose and sodium chloride, Standard; rhodamine 6G, fluorescein diacetate (FDA), KTC, clotrimazole, cycloheximide, 4-nitroquinoline-*N*-oxide (4-NQO), and RPMI 1640, Sigma; and morpholinepropanesulfonic acid (MOPS), Amresco. The synthesis of the aminophenothiazine maleates M942, M959, M960, M961, M962, and M963 was carried out as described previously (35). Thioridazine and trifluoperazine were obtained from ICN. Amineptine, dextromepromazine, diethazine, levomepromazine, and thietilperazine were kindly provided by J. Molnar. Other phenothiazine derivatives, including fluphenazine, were obtained from Sigma.

**Plasmid construction.** The plasmid pKV2MK was constructed by homologous recombination of the SapI-XhoI fragment of pKV2 (22) with the PCR-amplified fragment of pRS316 (52), using the primers TCCATTATGTACTATTTAAAA AACACAACTTTGGATGTTTCGGTTTATTGGTCTTTTCATCACGTGCTATAA and AACGCGGCTTTTACGGTTCCTGGCCTTTTGTGGCC TTTTGTCTACATGGGTAATAACTGATATAATTAATTGAAGCTC.

The SacI-XbaI fragment of pDDB57 (60), containing the *CaURA3* cassette, and the PmeI-BglII fragment of pFA6-3HA-His3MX6 (31), containing the *HIS3MX6* cassette, were treated with the DNA polymerase I large (Klenow) fragment and inserted at several places into the *PDR5* promoter fused with the  $\beta$ -galactosidase reporter in pKV2MK. The resulting constructs were verified for orientation and assayed for  $\beta$ -galactosidase activity after transformation into the hyperactivating *PDR1-3* regulatory mutant strain, using ONPG (*o*-nitrophenyl- $\beta$ -D-galactopyranoside) as a substrate, as previously described (17). A construct with an insertion of *CaURA3* that retained the full activity of the intact *PDR5* promoter was selected for further modifications.

Next, an internal deletion was introduced by the ExSite procedure (Stratagene), using the primers GGACGGATCGCTTGCCCTGTAAC and TGTGAGC AAAAGGCCAGCAAAG, and the SmaI fragment was removed from the resulting clone to obtain pMK5.

The region encoding the C-terminal part of Pdr5p and the terminator region were PCR amplified in two steps, with concomitant insertion of a 10-histidine tag. In the first step, fragment 1 was generated with the primers ATTAAGCTTGCTAGAA TTCACACCACCAT and CCAAATTCAAAATCTATTAGTGATGGTGATG GTGATGGTGATGGTGATGAGAACCCTTTCTGGAGAGTTTACCCTTCTT TTAGGC. Fragment 2 was amplified with primers TAATAGAATTTTGAATT TGGTTAAGAAAAGAAAC and GTGATGAAAAGGACCTAACTATATCCA TTGCGTC. After gel purification, fragments 1 and 2 were mixed and amplified in a second round with the flanking primers. The product was digested with HindIII and cloned into the HindIII and PmlI sites of pMK5 to generate pMK5h. The HindIII-PciI fragment of the pDR3.3 plasmid (29), encompassing the *PDR5* open reading frame, was cloned into pMK5h, resulting in pMKPDR5h. pMKCDR1h and pMKSNQ2h (Fig. 1) were obtained by homologous recombination of PCR-amplified *CDR1* and *SNQ2* with linearized pMK5h. The resulting clones were verified by sequencing.

**Strains and growth conditions.** The isogenic *S. cerevisiae* strains used in this study are listed in Table 1. To construct AK100, a deletion of *PDR5* was generated with the *URA3MX* cassette, generated by the adaptamer-mediated PCR procedure (45). Briefly, fragments 1 and 2 were amplified by PCR on the *PDR5* promoter and terminator regions, using the following primer pairs: for fragment 1, TTAACGTA AATATGCTTCTCTTTGATTCC and ACGACAACCTCAGCATCATGGCA TGAGGAACGTTTCATGTTCTTTATTAG; and for fragment 2, GTGTTTAGG TCGATGCCATCTTTGACTAGAAATTTGAATTTGGTTAAGAAAAG and TAACTATATCCATTGCGTCTTTCTT. Fragments 3 and 4 were amplified from the pAG61 plasmid (16) by using the following primer pairs: for fragment 3, TGC CATGATGCTGAAGTTGTCGT and CCCTCTGGCTCTTGGTTGGT; and for fragment 4, GCCTCACCAGTAGCACAACGATTATTT and GTACAAAGATG GCATCGACCTAAACAC. The PCR products were gel purified, and two additional PCRs were performed with the flanking primers, using combined fragments 1 and 3 as well as fragments 2 and 4 as templates. The two overlapping generated PCR products, 1+3 and 2+4, were cotransformed into the FYAK 26/8-4D2 strain by the lithium acetate procedure (15). The correct integration was verified by replica plating on medium containing cycloheximide and by colony PCR. The *URA3* gene was removed by 5-fluoroorotic acid treatment of the appropriate transformants (2).

MKCDR1h, MKPDR5h, and MKSNQ2h were obtained by integration of the gel-purified fragments of pMKCDR1h, pMKPDR5h, and pMKSNQ2h, respectively, into AK100 by homologous recombination and selection for uracil prototrophy. The resulting clones were verified by replica plating on medium containing cycloheximide, clotrimazole, and 4-NQO and by colony PCR.

To construct MKSNQ2, the *PDR5* promoter region of pMKPDR5h was

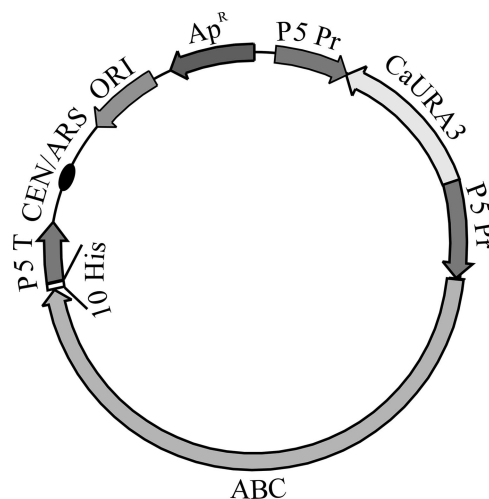


FIG. 1. Scheme of final constructs pMKCDR1h, pMKPDR5h, and pMKSNQ2h, used for overexpression and integration of the polyhistidine-tagged ABC transporters *CDR1*, *PDR5*, and *SNQ2* (ABC), respectively, under the control of the *PDR5* promoter (P5 Pr). The positions of the origin of replication in *Escherichia coli* (ORI), the ampicillin resistance gene ( $Ap^R$ ), the yeast centromere and autonomously replicating sequence (CEN/ARS), the *C. albicans URA3* gene, the polyhistidine tag (10 His), and the *PDR5* terminator (P5 T) are marked.

amplified with the primers ATTACATTCTCAGTGCATCCATCGTCTTCAACA TTGATTACCACCTTTGATTGTAATAGTAATAATTACCACCC and CAT TATGAGAGCTATCTTGCCTGCTTTTGTATTTGCTCATTTTTGTCTA AAGTCTTTTGAACGAGCGGATACG and integrated into the genome of FYAK 26/8-5A2, replacing the *SNQ2* promoter. The resulting clones were selected for uracil prototrophy and verified by replica plating on medium containing 4-NQO and by colony PCR. Similar drug resistance phenotypes were observed for FYAK 26/8-4D2 and MKPDR5h and for MKSNQ2 and MKSNQ2h, indicating that the presence of the 10-His epitope at the C terminus did not affect the function of the tagged proteins. This is in agreement with other studies in which C-terminal fusion with the even larger protein green fluorescent protein did not compromise the function of the MDR transporters Pdr5p (53; our unpublished observations) and Cdr1p (51). *C. albicans* isolate 15 (59) was kindly provided by Theodore White.

The MICs for *Candida* were determined by a microdilution assay in MOPS-buffered RPMI 1640 medium as previously described, using the CLSI M27-A broth microdilution method (38). MICs for *S. cerevisiae* were determined by a microdilution assay essentially as previously described (26). Growth was monitored by measuring the optical density at 550 (OD<sub>550</sub>) and OD<sub>600</sub> in a microplate reader as well as by visual inspection after 24 and 48 h. Compounds were added as dimethyl sulfoxide stock solutions, and an identical solvent amount was added to the control cultures, where it did not affect growth at the applied concentrations, not exceeding 1.2%. The MICs represent the values observed in three independent measurements in which the error did not exceed the window determined by the serial dilution factor. For the MIC breakpoint, the lowest concentration of compound that inhibited the growth yield by at least 80% compared to the drug-free control was used.

The effect of the combination of M961 or fluphenazine with KTC was determined by a microdilution checkerboard procedure (11). The FIC<sub>index</sub> was defined following the equation  $FIC_{index} = FIC_A + FIC_B = (MIC_{A\ comb}/MIC_{A\ alone}) + (MIC_{B\ comb}/MIC_{B\ alone})$ , where  $MIC_{A\ alone}$  and  $MIC_{B\ alone}$  are the MICs of drugs acting alone and  $MIC_{A\ comb}$  and  $MIC_{B\ comb}$  are MICs of drugs A and B in combination. Drug interactions were defined as synergistic if the FIC<sub>index</sub> was  $\leq 0.5$ , indifferent if the FIC<sub>index</sub> was  $> 0.5$  and  $\leq 4.0$ , and antagonistic if the FIC<sub>index</sub> was  $> 4$  (40, 58).

**Plasma membrane isolation.** Isolation of plasma membranes was performed according to the glass bead lysis procedure (10), with minor modifications as described previously (27). Membranes were analyzed by sodium dodecyl sulfate (SDS)-polyacrylamide gel electrophoresis in a Laemmli system (28) and stained with Coomassie brilliant blue R-250 (Bio-Rad).

TABLE 1. *Saccharomyces cerevisiae* strains used in this study

Strain	Genotype	Reference or source
FY1679-28C	<i>MATa ura3-52 trp1Δ63 leu2Δ1 his3Δ200 GAL2<sup>+</sup></i>	C. Fairhead
FYMK-1/1	<i>MATa ura3-52 trp1Δ63 leu2Δ1 his3Δ200 GAL2<sup>+</sup> pdr5-Δ1::hisG</i>	25
FYMK 23/2	<i>MATa ura3-52 trp1Δ63 leu2Δ1 his3Δ200 GAL2<sup>+</sup> snq2-Δ1::hisG</i>	25
FYMK 26/8-10B	<i>MATa ura3-52 trp1Δ63 leu2Δ1 his3Δ200 GAL2<sup>+</sup> pdr5-Δ1::hisG snq2-Δ1::hisG</i>	25
FYMK 26/8-5C	<i>MATa ura3-52 trp1Δ63 leu2Δ1 his3Δ200 GAL2<sup>+</sup> PDR1-3</i>	25
FYAK 26/8-4D2	<i>MATa ura3-52 trp1Δ63 leu2Δ1 his3Δ200 GAL2<sup>+</sup> PDR1-3 snq2-Δ1::hisG yor1-1::hisG</i>	A. Kolaczowska
FYAK 26/8-5A2	<i>MATa ura3-52 trp1Δ63 leu2Δ1 his3Δ200 GAL2<sup>+</sup> PDR1-3 pdr5-Δ1::hisG yor1-1::hisG</i>	A. Kolaczowska
AK100	<i>MATa ura3-52 trp1Δ63 leu2Δ1 his3Δ200 GAL2<sup>+</sup> PDR1-3 pdr5-Δ4::rep500 snq2-Δ1::hisG yor1-1::hisG</i>	This study
MKCDR1h	<i>MATa ura3-52 trp1Δ63 leu2Δ1 his3Δ200 GAL2<sup>+</sup> PDR1-3 pdr5-Δ4::CDR1h snq2-Δ1::hisG yor1-1::hisG</i>	This study
MKPDR5h	<i>MATa ura3-52 trp1Δ63 leu2Δ1 his3Δ200 GAL2<sup>+</sup> PDR1-3 pdr5-Δ4::PDR5h snq2-Δ1::hisG yor1-1::hisG</i>	This study
MKSNQ2h	<i>MATa ura3-52 trp1Δ63 leu2Δ1 his3Δ200 GAL2<sup>+</sup> PDR1-3 pdr5-Δ4::SNQ2h snq2-Δ1::hisG yor1-1::hisG</i>	This study
MKSNQ2	<i>MATa ura3-52 trp1Δ63 leu2Δ1 his3Δ200 GAL2<sup>+</sup> PDR1-3 snq2::pdr5prom pdr5-Δ1::hisG yor1-1::hisG</i>	This study

**Immunological methods.** Protein extracts were prepared by glass bead lysis as previously described (21). Protein concentrations were determined by use of a Bio-Rad protein assay kit as recommended by the supplier. Equal amounts of protein were resuspended in SDS loading buffer prior to analysis by Western blotting (56). Blots were incubated with India HisProbe-HRP (Pierce) and anti-Vph1p antibody (Molecular Probes) and developed with SuperSignal West Pico chemiluminescent substrate (Pierce).

**Fluorescence intensity measurements and calculations of results.** Exponentially growing cultures were collected and washed with water. Serial dilutions of the compounds to be tested were prepared in 96-well microtiter plates in 50 mM glucose-containing MOPS, pH 7. Next, the cell suspension was added, and the plates were preincubated for 5 min at room temperature. The reaction was started by the addition of FDA. Fluorescence intensity was recorded with Molecular Devices Gemini EM and XS microplate spectrofluorometers at 485-nm excitation and 538-nm emission wavelengths. The reaction rates, corresponding to the slopes of the linear fluorescence intensity traces recorded in real time, were calculated by the SoftmaxPro program, using linear fitting. To quantify the effects of different inhibitors, the reaction rates were plotted against the concentrations of each compound to generate dose-response curves. To avoid the influence of nonspecific effects which might result from the toxicity of the compounds at high concentrations, a new parameter, the concentration of inhibitor resulting in a threefold increase in the reaction rate over the background in the presence of solvent alone ( $IC_{3b}$ ), was calculated, after fitting of the curves to a polynomial, and used as a measure of inhibitor potency.

Measurements of inhibition of Pdr5p-mediated rhodamine 6G transport in isolated plasma membranes were performed with a Molecular Devices Gemini XS microplate spectrofluorometer, essentially as previously described (27), after adaptation to the 96-well microplate format. Briefly, serial dilutions of inhibitors in assay buffer were prepared in a 96-well microplate. Isolated plasma membranes and rhodamine 6G were then added. The reaction was started by the addition of Mg-ATP after 5 min of preincubation, and the fluorescence intensity was recorded in real time. The rates of rhodamine 6G fluorescence intensity decrease, corresponding to the slopes of the recorded traces in the linear region, were calculated using the SoftMax Pro program. The 50% inhibitory concentrations ( $IC_{50s}$ ) were calculated after fitting of the data with a four-parameter logistic equation.

## RESULTS

**Identification of a substrate suitable for high-throughput measurement of MDR transporter efflux activity in *S. cerevisiae*.** To identify substrates suitable for homogenous, real-time monitoring of the transport activity of MDR transporters in *S. cerevisiae*, we searched for compounds which change their fluorescence intensity upon accumulation in cells. We focused on a group of profluorochromes which become brightly fluorescent upon cleavage of the acetate or acetoxyethyl group by nonspecific intracellular esterases and produce a different signal in *S. cerevisiae* strains with disruptions in the major MDR

transporter genes *PDR5* and/or *SNQ2* compared with the wild-type reference signal.

Figure 2 reveals that the addition of FDA to the cell suspension of the wild-type FY1679-28C strain produced a slow linear increase in fluorescence intensity, which increased in the case of the otherwise isogenic *PDR5* disruptant (Table 1). A much higher rate of fluorescence intensity increase was observed with the double *PDR5 SNQ2* knockout, which indicated that both transporters modify the accumulation of FDA in cells. This effect was complemented by transformation of the plasmid-borne *PDR5* and/or *SNQ2* gene (data not shown). Introduction of the plasmid carrying the *CDR1* gene into the double *PDR5 SNQ2* knockout also caused a significant decrease in FDA accumulation (Fig. 2). Since much higher rates

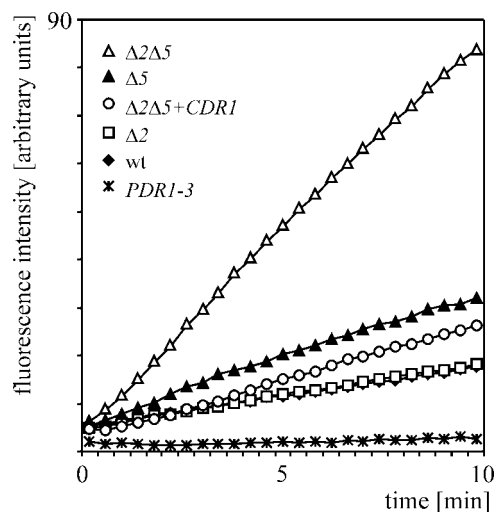


FIG. 2. Effects of Pdr5p, Snq2p, and Cdr1p on FDA accumulation in *S. cerevisiae*. Equal amounts of cells expressing different levels of the analyzed transporters were put into microplate wells, and the reaction, started by the addition of FDA, was monitored in a fluorescence reader in real time as described in Materials and Methods. The fluorescence intensity increase is proportional to the rate of intracellular accumulation. Disruptions in *PDR5* and *SNQ2* are indicated as  $\Delta 5$  and  $\Delta 2$ , respectively. The presence of a plasmid-carried *CDR1* gene is marked (+*CDR1*). The wild-type reference strain (wt) and the MDR regulatory *PDR1-3* mutant are indicated. The traces for the wild type and the *SNQ2* disruptant overlap.

of FDA hydrolysis and fluorescence signal generation, which were similar for all analyzed strains, were observed in glass bead-lysed cell suspensions (data not shown), this suggested that membrane penetration rather than intracellular FDA hydrolysis was the rate-limiting step. The deletion of *SNQ2* in the *PDR5* knockout, as expected, caused a larger increase in FDA accumulation than did deletion in the wild-type strain background. This was related to the much higher expression level of *PDR5*, which masks the *SNQ2*-related phenotypes (24, 32). The magnitude was further increased in the absence of *PDR5* due to the elevated expression of *SNQ2* by the compensatory transcriptional mechanism (24). The signal generated in the gain-of-function mutant of the transcriptional regulator gene *PDR1-3*, which contains elevated levels of Pdr5p and Snq2p in the plasma membrane due to hyperactivation of the corresponding *PDR5* and *SNQ2* promoters (6, 7), was, as expected, lower than that in the wild type and similar to that in the cell-free control (Fig. 2).

**Overproduction, normalization of transporter expression, and effect on FDA accumulation.** Cdr1p as well as Pdr5p and Snq2p was overproduced in order to reduce the possible contributions of other endogenous transporters and to achieve a high dynamic response of measurements required for inhibitor analysis. Since high-level overproduction of membrane proteins is often difficult to achieve due to toxicity and mislocalization issues, we used the *PDR5* promoter and the regulatory *PDR1-3* mutant, in which high levels of endogenous Pdr5p are properly targeted to the plasma membrane, leading to high-level MDR (7). Western blot analysis revealed that each of the C-terminally polyhistidine-tagged proteins was expressed in the host devoid of endogenous copies of *PDR5*, *SNQ2*, and *YOR1* (Fig. 3A). SDS-polyacrylamide gel electrophoresis confirmed the high levels of overproduction of polyhistidine-tagged Pdr5p, Snq2p, and Cdr1p in the plasma membranes, comparable to that of the marker enzyme Pma1p (Fig. 3B).

The drastic reduction in the rate of intracellular FDA accumulation upon overproduction of the analyzed transporters reached 50-fold, depending on the protein. It decreased from 8,123 (average value from 30 independent measurements; standard deviation [SD] = 487) in the expression host to 128 (SD = 10), 176 (SD = 14), and 159 (SD = 11) in the Cdr1p-, Pdr5p-, and Snq2p-overproducing strains, respectively. Thus, the similar levels of the analyzed transporters found in the plasma membranes were reflected by similar levels of FDA extrusion activity. The calculation of the *Z'* factor, which was equal to 0.8, indicated the high quality of the assay and its suitability for high-throughput screening (HTS) (62).

**Evaluation of assay performance and identification of new Cdr1p inhibitors showing different effects on Pdr5p and Snq2p.** To evaluate the performance of the new assay further and to identify new Cdr1p inhibitors, a series of closely related, therapeutically used, and newly synthesized phenothiazine derivatives was analyzed. The assay was performed in the presence of serial dilutions of test compounds and with *S. cerevisiae* strains MKCDR1h, MKPDR5h, and MKSNQ2h, selectively overproducing Cdr1p, Pdr5p, and Snq2p, respectively. It revealed gradual increases in the rate of intracellular FDA accumulation and the generation of the fluorescence signal above a certain concentration threshold (Fig. 4), which were not observed upon addition of the solvent alone. In contrast to

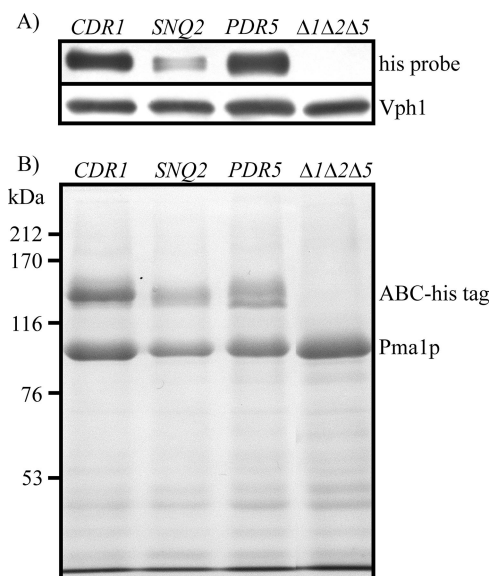


FIG. 3. Analysis of expression level and localization of overproduced polyhistidine-tagged transporters. (A) Western blot of cell extracts with the polyhistidine epitope-specific India HisProbe-HRP and with anti-Vph1p antibody as the loading control. (B) Coomassie-stained SDS-polyacrylamide gel showing plasma membrane fractions isolated from strains overproducing Cdr1p, Snq2p, and Pdr5p. The expression host, in which endogenous copies of *YOR1*, *SNQ2*, and *PDR5* were disrupted ( $\Delta 1\Delta 2\Delta 5$ ), served as a negative control. The positions of molecular size markers, histidine-tagged ABC transporters (ABC-His tag), and the plasma membrane marker enzyme proton ATPase Pma1p are indicated.

many enzymatic *in vitro* assays in which the saturation of the response is observed at higher inhibitor concentrations, a sudden drop in the rate of fluorescence intensity increase was often observed (data not shown). This phenomenon, which was related to the toxicity of the compounds at higher concentrations, did not allow for calculation of the  $IC_{50}$ . As evident from Fig. 4, however, large differences in the potencies of the inhibitors were observed in the initial regions of the dose-response curves. A new inhibitor of Cdr1p, M961, was active in the low micromolar range (Fig. 4). Three types of response were generally observed. M961, which was the most potent compound, turned out to be equally active against Cdr1p, Pdr5p, and Snq2p (Fig. 4A). In contrast, the three transporters differed in their responses to fluphenazine, which was most effective against Pdr5p. Cdr1p was the least sensitive to fluphenazine inhibition, whereas Snq2p showed an intermediate sensitivity (Fig. 4B). Snq2p, however, was specifically inhibited by phenothiazine, which was inactive against Cdr1p and Pdr5p (Fig. 4C). Since the decrease in the rate of the reaction was negligible at M961 concentrations below 0.01  $\mu$ M, as well as at fluphenazine and phenothiazine concentrations below 0.1  $\mu$ M, the corresponding data points were omitted from Fig. 4 for clarity.

To enable quantitative comparison of the inhibitors, we searched for parameters related to the initial regions of the dose-response curves.  $IC_{3b}$ , which is the concentration resulting in a threefold increase in the rate of fluorescence signal increase over the corresponding background in the absence of the inhibitor, was the most reproducible one. The standard

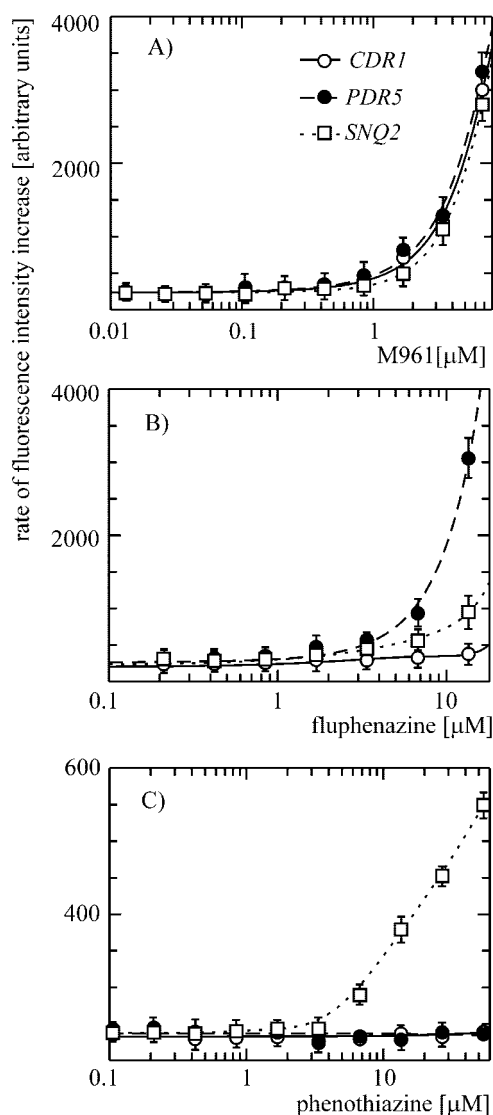


FIG. 4. Differential responses of Cdr1p, Pdr5p, and Snq2p to inhibition by phenothiazines in the newly developed fluorescence-based assay. Suspensions of *S. cerevisiae* cells specifically overproducing each of the three ABC MDR transporters (M961 [A], fluphenazine [B], and phenothiazine [C]) were added to serial dilutions of the compounds. The reaction was started by the addition of FDA, and its conversion to the free fluorescent form upon intracellular accumulation was measured in real time in a fluorescence microplate spectrophotometer as described in Materials and Methods.

deviation of  $IC_{3b}$  for five independent measurements was typically less than 10% of the measured value. It also showed the highest correlation with the results of the inhibitor potency measurements of other established assays. The mean values of  $IC_{3b}$  calculated for the tested series of compounds are summarized in Table 2, together with their structures.

**Comparison of the new assay with other methods.** The most common procedure for the initial evaluation of potential efflux pump inhibitors is measuring the ability of test compounds to potentiate the growth inhibitory effect of a toxic drug substrate of an MDR transporter. To verify whether the results of the new fluorescence-based assay correlate with those of a tradi-

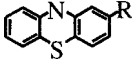




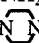
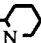
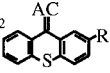
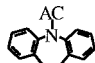
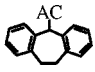
tional growth-based method, we searched for an antifungal drug substrate detoxified by the three analyzed transporters. There was a vast array of choices for both Pdr5p and Cdr1p, which decrease the intracellular concentrations of several azoles. Snq2p, however, has a more distinct specificity from those of Pdr5p and Cdr1p, with only some degree of overlap (25, 32). Figure 5A demonstrates that whereas the overproduction of Pdr5p and Cdr1p conferred similar levels of clotrimazole resistance, Snq2p did not detoxify this compound. This was also the case for several other azoles tested, indicating a much more limited specificity of this protein toward this class of drugs. In contrast, KTC was detoxified by all three proteins (Fig. 5B) (with MICs of 5  $\mu$ M for Pdr5p, 0.6  $\mu$ M for Cdr1p, and 0.3  $\mu$ M for Snq2p overproducers, compared to the MIC of the expression host of 0.01  $\mu$ M). We then measured MICs obtained in the presence of a subinhibitory concentration of KTC ( $MIC_{KTC}$ ), which was adjusted individually for each transporter-overproducing strain proportionally to the estimated MIC of this antifungal alone (2.5-fold below the MIC). The three types of responses observed in the growth assay shown in Fig. 6 for M961, fluphenazine, and phenothiazine reflected the relationships identified by the new fluorescence-based test (Fig. 4; Table 2).

Since the results of cell-based procedures can be affected by modification of additional cellular metabolic pathways in addition to MDR transport inhibition, we used a previously developed *in vitro* assay (27) to determine the  $IC_{50}$ s for phenothiazine inhibition of Pdr5p-mediated rhodamine 6G transport in isolated plasma membranes. Figure 7 shows a typical dose-response curve for the most potent inhibitor, M961, which was active in the nanomolar range.  $IC_{50}$ s for other compounds are summarized in Table 2.

The high levels of correlation of the  $IC_{3b}$  with  $MIC_{KTC}$  (Fig. 8A to C) and  $IC_{50}$  (Fig. 8E) values and also of  $IC_{50}$  with  $MIC_{KTC}$  (Fig. 8D) were revealed by scatter plot analysis and linear regression fitting of the data points after logarithmic conversion. The scatter plot of the log  $IC_{50}$  and log  $IC_{3b}$  values for Pdr5p revealed a distinct trend for the subpopulation of M series aminophenothiazine inhibitors (Fig. 8E; Table 2). When this subset of the most closely structurally related compounds was treated separately in the regression analysis, there was an increase in Pearson's correlation coefficient, from 0.86 ( $P < 0.0001$ ;  $r^2 = 0.73$ ) for all compounds to 0.92 ( $P < 0.007$ ;  $r^2 = 0.86$ ) for the M series and 0.93 ( $P < 0.0001$ ;  $r^2 = 0.86$ ) for the rest of the population. The log  $IC_{3b}$  and log  $MIC_{KTC}$  parameters for Cdr1p and Snq2p also showed high degrees of correlation ( $r = 0.91$ ,  $P < 0.0001$ , and  $r^2 = 0.83$  for Cdr1p and  $r = 0.92$ ,  $P < 0.0001$ , and  $r^2 = 0.85$  for Snq2p) (Fig. 8).

**Similarities and differences in phenothiazine derivative inhibitory potencies against Cdr1p, Pdr5p, and Snq2p.** The analysis of the  $IC_{3b}$  values for strains overproducing Cdr1p, Pdr5p, and Snq2p revealed the major influence of the acyl chain substituent at position 10 of the phenothiazine ring (the nitrogen atom) on their inhibitory activity. The most active compounds (M961 [compound 1] and M963 [compound 2]) (Fig. 9; Table 2) contained the primary amine group at the end of the butylene chains. Shortening them by one carbon atom decreased the potency, as seen with M942 (compound 3) and M962 (compound 9). The compounds containing a piperazinyl group (e.g., fluphenazine [compound 4] and trifluoperazine

TABLE 2. Parameters of in vitro and in vivo inhibition of the multidrug transporters Pdr5p, Cdr1p, and Snq2p by phenothiazines and related compounds

Compound no.	Name	R substituent <sup>a</sup>	Acyl chain 	Pdr5p IC <sub>50</sub> <sup>b</sup> (μM)	IC <sub>30</sub> (μM)			MIC <sub>KTC</sub> (μM)			Fold resistance <sup>c</sup>		
					Pdr-5p	Cdr-1p	Snq-2p	Pdr-5p	Cdr-1p	Snq-2p	Pdr-5p	Cdr-1p	Snq-2p
1	M961	Cl	CH <sub>2</sub> -CH <sub>2</sub> -CH <sub>2</sub> -CH <sub>2</sub> -NH <sub>2</sub>	0.7	1.9	1.9	2.1	1.4	1.4	1.4	2	2	2
2	M963	CF <sub>3</sub>	CH <sub>2</sub> -CH <sub>2</sub> -CH <sub>2</sub> -CH <sub>2</sub> -NH <sub>2</sub>	1.3	3.7	4.6	4.6	2.9	5.8	5.8	4	4	2
3	M942	Cl	CH <sub>2</sub> -CH <sub>2</sub> -CH <sub>2</sub> -NH <sub>2</sub>	3.2	4.2	4.3	5.8	2.9	5.8	5.8	2	2	1
4	Fluphenazine	CF <sub>3</sub>	CH <sub>2</sub> -CH <sub>2</sub> -CH <sub>2</sub> -  -CH <sub>2</sub> -CH <sub>2</sub> -OH	1.7	5.4	12.4	8.8	2.9	11.5	11.5	4	4	4
5	Thiethylperazine	S-CH <sub>2</sub> -CH <sub>3</sub>	CH <sub>2</sub> -CH <sub>2</sub> -CH <sub>2</sub> -  -N-CH <sub>3</sub>	2.3	5.6	9.4	3.2	2.9	11.5	2.9	2	4	2
6	Perphenazine	Cl	CH <sub>2</sub> -CH <sub>2</sub> -CH <sub>2</sub> -  -N-CH <sub>2</sub> -CH <sub>2</sub> -OH	1.4	6.4	17.2	13.1	2.9	11.5	5.8	2	2	2
7	M960	H	CH <sub>2</sub> -CH <sub>2</sub> -CH <sub>2</sub> -CH <sub>2</sub> -NH <sub>2</sub>	3.1	7.0	29	13.5	5.8	23	11.5	2	2	1
8	Prochlorperazine	Cl	CH <sub>2</sub> -CH <sub>2</sub> -CH <sub>2</sub> -  -N-CH <sub>3</sub>	1.7	7.2	11.0	6.6	2.9	5.8	2.9	2	4	2
9	M962	CF <sub>3</sub>	CH <sub>2</sub> -CH <sub>2</sub> -CH <sub>2</sub> -NH <sub>2</sub>	6.4	7.7	6.5	6.9	5.8	11.5	5.8	4	4	2
10	Trifluoperazine	CF <sub>3</sub>	CH <sub>2</sub> -CH <sub>2</sub> -CH <sub>2</sub> -  -N-CH <sub>3</sub>	1.4	8.3	9.8	6.9	2.9	11.5	2.9	2	4	2
11	M959	H	CH <sub>2</sub> -CH <sub>2</sub> -CH <sub>2</sub> -NH <sub>2</sub>	7.4	14.7	36	12.4	23	46	23	2	2	1
12	Thioridazine	S-CH <sub>3</sub>	CH <sub>2</sub> -CH <sub>2</sub> - 	1.3	17.0	26	19.4	2.9	11.5	5.8	4	8	2
13	Chlorprothixene	Cl	=CH-CH <sub>2</sub> -CH <sub>2</sub> -N-(CH <sub>3</sub> ) <sub>2</sub> 	5.1	26	53	22	5.8	11.5	5.8	1	2	1
14	Trifluopromazine	CF <sub>3</sub>	CH <sub>2</sub> -CH <sub>2</sub> -CH <sub>2</sub> -N-(CH <sub>3</sub> ) <sub>2</sub>	4.9	47	49	47	11.5	11.5	11.5	2	4	2
15	Chlorpromazine	Cl	CH <sub>2</sub> -CH <sub>2</sub> -CH <sub>2</sub> -N-(CH <sub>3</sub> ) <sub>2</sub>	4.5	57	57	32	5.8	11.5	11.5	2	4	2
16	Promazine	H	CH <sub>2</sub> -CH <sub>2</sub> -CH <sub>2</sub> -N-(CH <sub>3</sub> ) <sub>2</sub>	11.3	96	278	131	46	92	46	2	4	2
17	Dextromepromazine	O-CH <sub>3</sub>	CH <sub>2</sub> -CH(CH <sub>3</sub> )-CH <sub>2</sub> -N-(CH <sub>3</sub> ) <sub>2</sub>	9.0	101	273	100	46	92	46	4	4	1
18	Levomepromazine	O-CH <sub>3</sub>	CH <sub>2</sub> -CH(CH <sub>3</sub> )-CH <sub>2</sub> -N-(CH <sub>3</sub> ) <sub>2</sub>	9.6	128	252	100	46	92	46	4	4	1
19	Imipramine	H	CH <sub>2</sub> -CH <sub>2</sub> -CH <sub>2</sub> -N-(CH <sub>3</sub> ) <sub>2</sub> 	22	166	>433	198	92	184	92			
20	Promethazine	H	CH <sub>2</sub> -CH(CH <sub>3</sub> )-N-(CH <sub>3</sub> ) <sub>2</sub>	17.7	285	275	117	92	92	46	2	2	92
21	Diethazine	H	CH <sub>2</sub> -CH <sub>2</sub> -N-(CH <sub>2</sub> -CH <sub>3</sub> ) <sub>2</sub>	10.3	331	317	239	92	92	92	2		
22	Phenothiazine	H	H	>400	>433	>433	90	>368	>368	11.5			
23	Amineptine	H	NH-CH <sub>2</sub> -CH <sub>2</sub> -CH <sub>2</sub> -  -CH <sub>2</sub> -CH <sub>2</sub> -CH <sub>2</sub> -COOH	>400	>433	>433	>433	>368	>368	>368			

<sup>a</sup> Substituent at position 2 of the ring backbone.

<sup>b</sup> IC<sub>50</sub> for rhodamine 6G transport in isolated plasma membranes.

<sup>c</sup> Ratio of the MIC of the strain overproducing the indicated transporter to the MIC of the isogenic expression host.

[compound 10]) or piperidine (thioridazine [compound 12]) in their acyl chain followed. The phenothiazine derivatives containing a tertiary amine, including promazine, promethazine, and diethazine, were the least potent. The influence of the functional group at position 2 on inhibition (Fig. 9; Table 2) was highest in the most active aminophenothiazines. These contained a Cl atom, whereas substitution with CF<sub>3</sub> and H strongly decreased the inhibition potency in both series containing butylene or propylene acyl chains. The substituents at position 2 also had a strong influence on the sensitivity of particular transporters to inhibition. Whereas the derivatives containing Cl and CF<sub>3</sub> (M961 [compound 1], M942 [compound 3], M963 [compound 2], and M962 [compound 9]) inhibited Cdr1p, Pdr5p, and Snq2p with similar potencies, differences were observed with the H-substituted series compounds M960

(compound 7) and M959 (compound 11). M960 (compound 7) was the most potent inhibitor of Pdr5p, whereas Snq2p showed an intermediate sensitivity and Cdr1p was the least sensitive (Fig. 9). A different order of sensitivity, Cdr1p > Pdr5p > Snq2p, was observed with trifluoperazine (compound 10), prochlorperazine (compound 8), and thiethylperazine (compound 5), containing CF<sub>3</sub>, Cl, and S-CH<sub>2</sub>-CH<sub>3</sub> functional groups at position 2, respectively, with the last producing the largest difference (Fig. 9). Also, M959 (compound 11) was less effective against Cdr1p, whereas Snq2p and Pdr5p showed similar sensitivities. Patterns similar to that of M959 (compound 11) were observed with promazine (compound 16), prochlorperazine (compound 8), dextromepromazine (compound 17), levomepromazine (compound 16), and the structurally related dibenzazepine imipramine (compound 19) (Fig. 9), illustrating

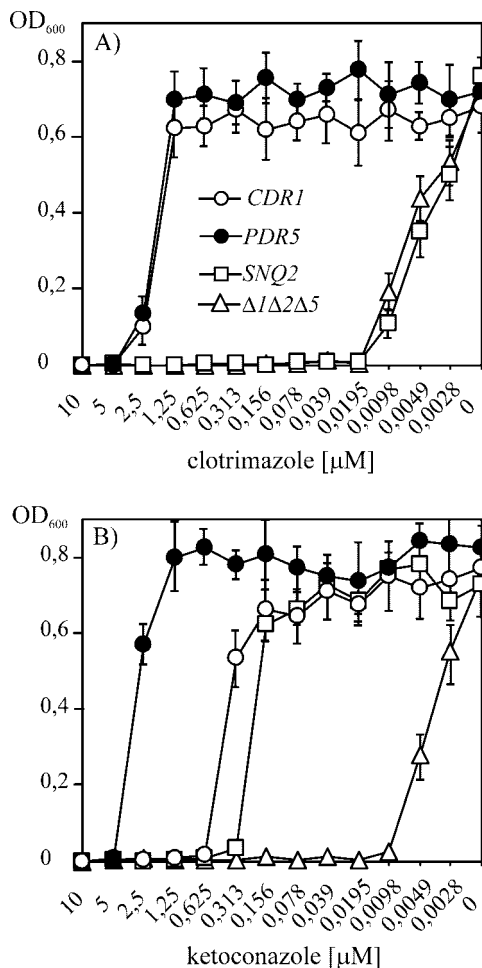


FIG. 5. Similarities and differences in azole resistance profiles for Cdr1p, Pdr5p, and Snq2p. Equal amounts of *S. cerevisiae* cells specifically overproducing each of the three ABC MDR transporters (designated in the legend in panel A) were inoculated into microplate wells containing serial twofold dilutions of clotrimazole (A) or KTC (B). Growth was monitored by OD<sub>600</sub> measurements on a microplate reader, as described in Materials and Methods.

that the combination of the acyl chain and the position 2 substituent affects the preference toward a particular transporter.

**M961 potentiates KTC antifungal activity against the resistant Cdr1p-overproducing *C. albicans* isolate better than fluphenazine does.** To verify whether the newly identified and most potent Cdr1p inhibitor M961 shows activity against *C. albicans*, its effect against an MDR Cdr1p-overproducing isolate was verified. It was also compared in parallel with fluphenazine, which has previously been shown to potentiate the antifungal effect of fluconazole (33). The checkerboard assay comparing the effects of KTC and inhibitor alone and those of both compounds in combination allowed us to calculate the corresponding fractional inhibitory concentration (FIC) and FIC<sub>index</sub> values (11, 58). The MIC of KTC alone of 0.92  $\mu\text{M}$  decreased to 0.03  $\mu\text{M}$  in the presence of M961 and to 0.06  $\mu\text{M}$  in the presence of fluphenazine. The MIC of M961 alone of 74.6  $\mu\text{M}$  decreased to 2.3  $\mu\text{M}$  in the presence of KTC, whereas the MIC of fluphenazine alone of 149.3  $\mu\text{M}$  decreased to 4.7

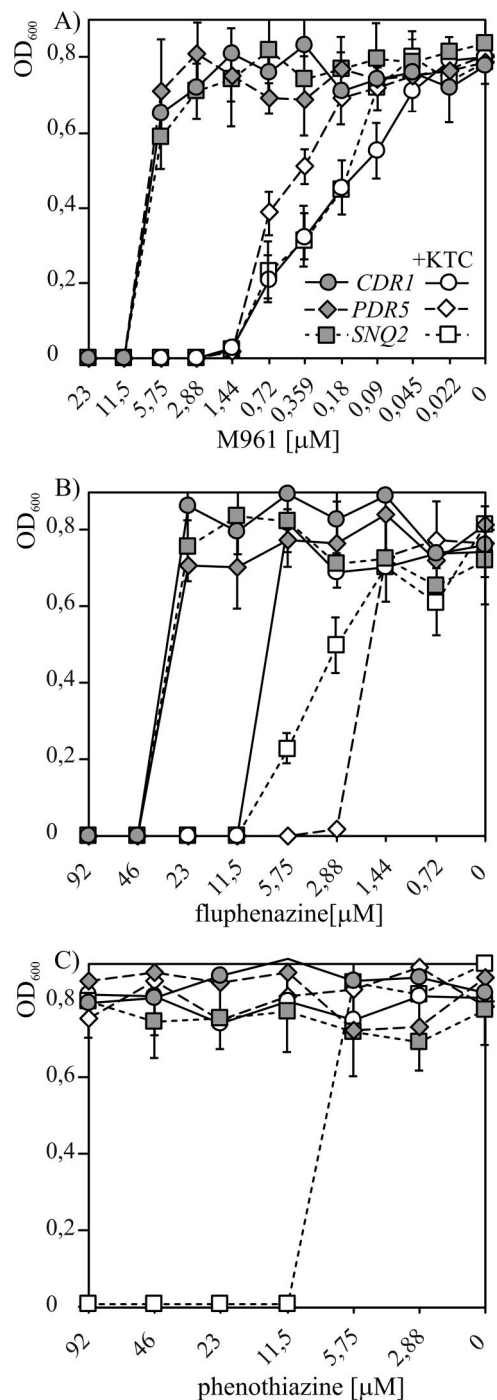


FIG. 6. Effects of identified inhibitors of FDA transport by Cdr1p, Pdr5p, and Snq2p on the reversal of KTC resistance mediated by these three transporters. Equal amounts of *S. cerevisiae* cells specifically overproducing each of the three ABC MDR transporters (designated in the legend in panel A) were inoculated into microplate wells containing serial twofold dilutions of the specified inhibitors (M961 [A], fluphenazine [B], and phenothiazine [C]) applied alone (shaded symbols) or combined with a subinhibitory KTC concentration (+KTC) (open symbols), adjusted for each strain to be 2.5-fold below the MIC. Growth was monitored by OD<sub>600</sub> measurements on a microplate reader, as described in Materials and Methods.

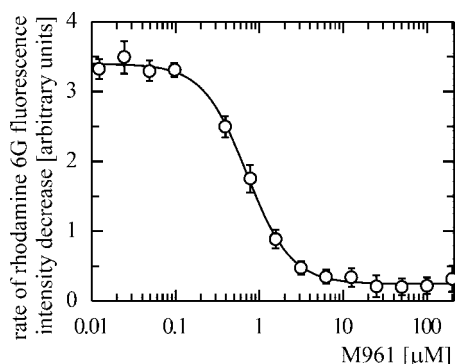


FIG. 7. Dose-response curve for M961 inhibition of Pdr5p-mediated rhodamine 6G transport in isolated plasma membranes. Serial dilutions of M961 in assay buffer in a 96-well microplate were prepared. Isolated plasma membranes and rhodamine 6G were then added. The reaction was started by Mg-ATP addition, and the fluorescence intensity was recorded in real time as described in Materials and Methods. The rate of rhodamine 6G fluorescence intensity decrease was plotted versus M961 concentration. The  $IC_{50}$  of 0.7  $\mu$ M was calculated after fitting of the data with a four-parameter logistic equation.

$\mu$ M. The corresponding  $FIC_{index}$  values for M961 (0.06) and fluphenazine (0.09) indicated a synergistic interaction with KTC for both compounds (40). The lower  $FIC_{index}$  observed for M961 than that for fluphenazine was in agreement with the higher potency of Cdr1p inhibition observed in the new *S. cerevisiae*-based fluorescence assay.

## DISCUSSION

In this study, we developed and characterized a new fluorescence-based assay allowing the fast, precise, and economical measurement of MDR efflux pump inhibition in whole cells upon overproduction in *S. cerevisiae*. It is based on a compound's ability to interfere with MDR transporter-mediated extrusion of FDA from the plasma membrane, leading to increased intracellular accumulation. This resulted in an increase in fluorescence intensity due to cleavage by intracellular esterases, which was measured homogeneously in whole cells in real time and quantified. The assay allowed the identification of new inhibitors of Cdr1p, the major MDR pump of the important human fungal pathogen *C. albicans*, and for rapid comparison of their effects on related MDR transporters.

Target-oriented screening of MDR transporter inhibitors in *S. cerevisiae* is an attractive alternative to screening in related pathogenic yeasts, thanks to the better knowledge of the network of pleiotropic drug resistance genes and the ease of genetic manipulation in this organism, which for many years served as a model eukaryote. This knowledge was important for reduction of the background of the most prominent interfering endogenous MDR efflux activities by deletion and for increasing the sensitivity and dynamic range of the assay by overproduction of target transporters in plasma membranes. *S. cerevisiae* has successfully been used in the past for HTS applications upon heterologous expression of target proteins (36). The high-level functional expression of several drug transporters from pathogenic fungi as well as those responsible for human cancer cell resistance to chemotherapy has also

been achieved in this organism, with proper targeting to the plasma membrane (12, 37). Finally, this approach combined with traditional growth-based screening resulted in the identification of most of the few known efflux pump inhibitors that are active against pathogenic fungi (39, 54).

The availability of previously developed methods for measurement of endogenous MDR transporter activities, in particular the rhodamine 6G transport assay for Pdr5p in the isolated plasma membrane fractions (27), and knowledge of the drug resistance profiles of Pdr5p and Snq2p (25) were additional advantages allowing for comparison of the new assay with established procedures.

The advantage of the new whole-cell assay format over measurements at the subcellular level lies in its simplicity and ease of manipulation, as it does not require preparations which are laborious, costly, and often difficult to perform on a large scale. This is of particular importance in initial screening steps and when rapid comparison of the effects of inhibitors on multiple MDR transporters or their variants is needed. It also allows the elimination of potential lead compounds which cannot be used due to low penetration or instability in cells.

The advantages of the new assay over other methods traditionally used for the characterization of MDR transporter inhibitors with whole cells, which are mainly based on the ability of tested compounds to potentiate the action of the effluxed cytotoxic drug on growth (14, 34), include reduced time and handling as well as increased precision. This was achieved thanks to a high sensitivity, dynamic range, and real-time detection without the necessity to separate cells from the reaction mixture, in contrast to methods employing radiolabeled or other fluorescent substrates, including anthracyclines and rhodamine derivatives (3, 23, 24, 27).

In the search for MDR transporter substrates allowing for more sensitive fluorescence-based detection in *S. cerevisiae*, we found that Pdr5p and Snq2p decrease the intracellular accumulation of FDA. This profluorochrome was previously found to diffuse through the plasma membrane into *S. cerevisiae* cells, where it was hydrolyzed to free fluorescein by esterases, whose activity was constant during culture growth (4). Our finding was unexpected based on the previous observation that this process did not depend on the MDR modulators reserpine and verapamil (4), but a clear increase in intracellular FDA accumulation was observed upon deletion of the endogenous MDR transporter genes *PDR5* and *SNQ2*. This effect was complemented by corresponding plasmid-borne genes and also by *CDR1* of *C. albicans*, which was in agreement with the observation by Yang et al. (61) that this transporter affects FDA accumulation in *C. albicans*. This indicated that FDA may be a universal substrate suitable for HTS measurement of inhibition of multiple MDR efflux pumps significantly differing in their resistance spectra in *S. cerevisiae*. The high dynamic response of the assay achieved upon overproduction of Cdr1p, Pdr5p, or Snq2p from a common promoter in a host devoid of endogenous copies of *PDR5*, *SNQ2*, and *YOR1* is comparable to that observed with calcein-AM, which is used to monitor the activity of the human MDR efflux pumps P-glycoprotein ( $ABC^{B1}$ ) and MRP ( $ABC^{C1}$ ) expressed in the mammalian system (19, 49), and largely exceeds those observed with other known procedures.

The series of closely related phenothiazine derivatives was



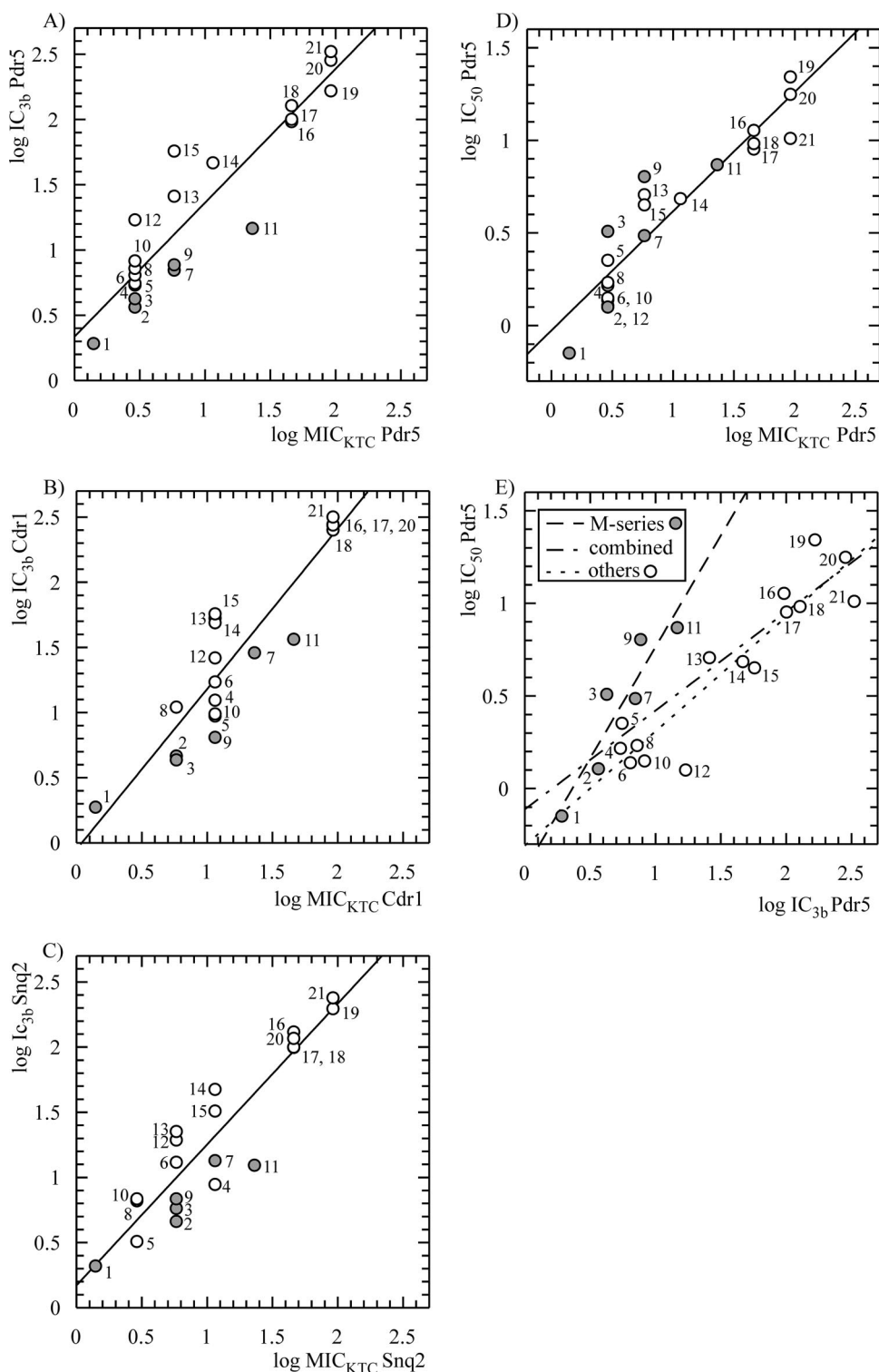


FIG. 8. Correlation of parameters of inhibition of MDR transporters Pdr5p, Cdr1p, and Snq2p by a series of phenothiazines and related molecules obtained in the new HTS assay with those measured by previously established procedures. (A to C) Scatter plots of logarithms of  $MIC_{KTC}$  values (MICs obtained in the presence of a subinhibitory KTC concentration) versus logarithms of  $IC_{3b}$  (inhibitor concentration resulting in a threefold increase in the fluorescence signal over the background) (Table 2). A linear fit with Pearson's correlation coefficient of 0.92, a  $P$  value of  $<0.0001$ , and a coefficient of determination of 0.85 is presented for Pdr5p. The correlations for Cdr1p ( $r = 0.91$ ,  $P < 0.0001$ , and  $r^2 = 0.83$ ) and Snq2p ( $r = 0.92$ ,  $P < 0.0001$ , and  $r^2 = 0.85$ ) are also shown. (D) Scatter plot of logarithms of  $MIC_{KTC}$  values versus logarithms of  $IC_{50}$ s for inhibition of Pdr5p-mediated rhodamine 6G transport in isolated plasma membranes. A linear fit with a correlation coefficient of 0.92, a  $P$  value of  $<0.0001$ , and an  $r^2$  value of 0.85 is shown. (E) Scatter plot of logarithms of  $IC_{3b}$  values versus logarithms of  $IC_{50}$ s. Linear fits with the combined set of data ( $r = 0.86$ ,  $P < 0.0001$ , and  $r^2 = 0.73$ ) and with two subsets of compounds showing close structural similarity within the subgroup, i.e., the M series (gray dots) ( $r = 0.93$ ,  $P < 0.007$ , and  $r^2 = 0.86$ ) and others (white dots) ( $r = 0.93$ ,  $P < 0.0001$ , and  $r^2 = 0.86$ ), are shown. Number designations correspond to those in Table 2, summarizing the structures of the compounds.

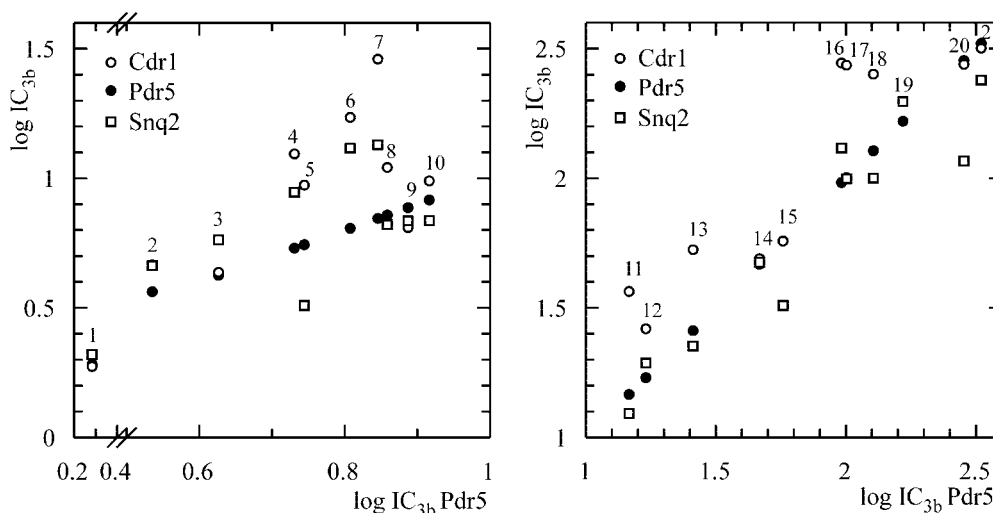


FIG. 9. Similarities and differences in responses of MDR transporters Pdr5p, Cdr1p, and Snq2p to inhibition by a series of phenothiazines and related molecules. The scatter plots show the logarithms of the  $IC_{3b}$  values (inhibitor concentration resulting in a threefold increase in the fluorescence signal over the background) measured in the new HTS assay for Pdr5p versus those for Cdr1p and Snq2p as well as those for Pdr5p itself (following the equity line). The closer to the equity line a data point is for Snq2p and Cdr1p (vertically), the more similar is its effect to that exerted on Pdr5p. More potent inhibitors with lower  $log IC_{3b}$  values are in the lower left corner, and the less potent inhibitors are in the upper right corner. The graph is split into two parts for better data point visibility. The scaling for the vertical axes is the same. Number designations correspond to those in Table 2, summarizing the structures of the compounds.

chosen to evaluate the assay's performance due to their ability to reverse MDR resistance in bacterial (20), cancer (13, 44), and yeast (26) cells. Although fluphenazine was previously shown to potentiate the effect of fluconazole on *C. albicans*, the activities of other phenothiazines, including several new ones against Cdr1p as well as Snq2p, were not tested so far. Snq2p was included to verify the assay performance with MDR transporters with significantly different resistance profiles, and the specificities of Pdr5p and Snq2p of *S. cerevisiae* are the best described, to our knowledge, among those of yeast MDR transporters (25). The analysis revealed several new inhibitors of Cdr1p, with the most potent aminoacyl derivative, M961, acting in the low micromolar range. It also showed similarities and differences in the inhibition profiles of the transporters Cdr1p, Snq2p, and Pdr5p, thanks to their similar expression levels found in plasma membranes and similar FDA extrusion activities. The most spectacular difference was in the response to phenothiazine, which specifically inhibited Snq2p with no effect on Pdr5p and Cdr1p. Similar differential responses were observed in the traditional growth assay, based on the potentiation of the antifungal effect of KTC, which was detoxified to similar extents by the three analyzed transporters. These differential effects were not related to the differential toxicity of the analyzed phenothiazines, as the analyzed strains did not differ in their susceptibility to compounds differently potentiating the response of Cdr1p-, Pdr5p-, and Snq2p-overproducing strains to KTC, such as M961, fluphenazine (Fig. 6), or phenothiazine, which did not inhibit yeast growth at all.

Interestingly, the overproduced transporters conferred a low level, usually two- to fourfold, of resistance to most analyzed phenothiazines (Table 2). This, together with their differential effect on tested transporters, indicated that these phenothiazines are poorly translocated substrates interacting with the transported drug-binding sites. The structural similarity of the

specific Snq2p inhibitor phenothiazine to specific Snq2p substrates, such as 4-NQO, phenanthroline (50), and resazurine (25), further supports this view. Finally, these compounds inhibited Pdr5p-mediated rhodamine 6G transport in isolated plasma membrane fractions. This assay is unique in its performance, allowing for detailed characterization of Pdr5p inhibitors (5, 27), and similar procedures with subcellular fractions have not been described for other fungal MDR transporters. Although we tried to adapt this method for measuring inhibition of Cdr1p activity in the microplate format, the lower dynamic range in this setup than that with Pdr5p did not allow for a large-scale analysis. This was in agreement with the lower level of rhodamine 6G resistance conferred by Cdr1p in growth assays (data not shown). The ability to inhibit Pdr5p-mediated rhodamine 6G transport in isolated plasma membranes was previously shown to be related to direct binding to the protein for a series of prenyl flavonoids (5). The direct phenothiazine binding to the NorA MDR transporter of *Staphylococcus aureus* as well as to the human P-glycoprotein has been suggested to make an important contribution to inhibition of these efflux pumps (20, 30). A point mutation in P-glycoprotein has also been shown to affect the interaction with the thioxanthenes *cis*- and *trans*-flupentixol, which are structurally closely related to phenothiazines (9).

The ability of Cdr1p, Pdr5p, and Snq2p to extrude FDA directly from the plasma membrane before it reaches the cytoplasm indicates that the transported substrates are recognized while crossing the membrane. Thus, the membrane interactions of substrate-resembling inhibitors should be an important factor affecting their activity. However, analysis of the most potent inhibitors, the aminophenothiazines (M series), revealed a different order of potency from that suggested by their liposome-buffer partition coefficients. Similarly, the inhibition of P-glycoprotein did not correlate with lipophilicity

and the membrane-perturbing potency of these compounds (18), pointing to the importance of their specific interactions with drug efflux pumps.

The new parameter IC<sub>3b</sub>, the inhibitor concentration causing a threefold increase in fluorescence signal over the background, was identified as a quantitative measure of the inhibition potency in the new assay, as estimation of IC<sub>50</sub>s was not possible because the plateau in the dose-response curves could not be obtained in most cases due to toxicity. Although a similar approach to quantifying P-glycoprotein inhibitor potency with the calcein-AM assay was attempted, the concentration causing a twofold increase over the background (f2) was used (57). The availability of alternative methods of inhibitor potency measurements with the *S. cerevisiae* expression system, such as the traditional growth-based assay with a sub-inhibitory KTC concentration and, in particular, the precise method of IC<sub>50</sub> measurement of Pdr5p-mediated rhodamine 6G transport inhibitors with isolated plasma membranes (27), allowed for correlation analysis of the results obtained by the three approaches. The IC<sub>3b</sub> values not only proved more reproducible than concentrations causing a twofold increase but also showed a higher level of correlation with the results of other methods.

The CgSnq2p protein of *Candida glabrata*, a homologue of the *S. cerevisiae* protein Snq2p, was recently shown to confer resistance to 4-NQO, fluconazole, and KTC (55). Our observation that Snq2p confers a level of KTC resistance similar to that by Cdr1p upon normalization of the expression level, although its specificity for other azoles, such as clotrimazole, is more limited, is important for the treatment of *C. glabrata*, which generally shows low azole susceptibility. Identification of a phenothiazine as a specific Snq2p inhibitor indicates the possible use of its close structural derivatives in increasing the potency of azoles against *C. glabrata*.

The identification of M961 as a new Cdr1p inhibitor that is more effective than fluphenazine in potentiating the antifungal effect of KTC on *C. albicans* demonstrates the predictive power of the new HTS assay. This method is an important new tool which should make a significant contribution to the identification of new inhibitors of drug efflux pumps of clinical importance to fight the threat of MDR pathogens.

#### ACKNOWLEDGMENTS

We are grateful to Antoni Polanowski and Jacek Otlewski for sharing laboratory equipment, to Scott Moye-Rowley for sharing equipment and materials, to Theodore White for the *Candida albicans* isolate, and to Joseph Molnar for the gift of amineptine, dextrometopromazine, diethazine, levomepromazine, and thietilperazine.

This work was supported by the Ministry of Science and Higher Education grant 2P05A 080 28 and by funds from the Wrocław Medical University.

#### REFERENCES

- Balzi, E., M. Wang, S. Leterme, L. Van Dyck, and A. Goffeau. 1994. PDR5, a novel yeast multidrug resistance conferring transporter controlled by the transcription regulator PDR1. *J. Biol. Chem.* **269**:2206–2214.
- Boeke, J. D., F. LaCroute, and G. R. Fink. 1984. A positive selection for mutants lacking orotidine-5'-phosphate decarboxylase activity in yeast: 5-fluoro-orotic acid resistance. *Mol. Gen. Genet.* **197**:345–346.
- Bosch, I., C. L. Crankshaw, D. Piwnica-Worms, and J. M. Croop. 1997. Characterization of functional assays of multidrug resistance P-glycoprotein transport activity. *Leukemia* **11**:1131–1137.
- Breuer, P., J. L. Drocourt, N. Bunschoten, M. H. Zwietering, F. M. Rombouts, and T. Abee. 1995. Characterization of uptake and hydrolysis of fluorescein diacetate and carboxyfluorescein diacetate by intracellular esterases in *Saccharomyces cerevisiae*, which result in accumulation of fluorescent product. *Appl. Environ. Microbiol.* **61**:1614–1619.
- Conseil, G., A. Decottignies, J. M. Jault, G. Comte, D. Barron, A. Goffeau, and A. Di Pietro. 2000. Prenyl-flavonoids as potent inhibitors of the Pdr5p multidrug ABC transporter from *Saccharomyces cerevisiae*. *Biochemistry* **39**:6910–6917.
- Decottignies, A., L. Lambert, P. Catty, H. Degand, E. A. Epping, W. S. Moye-Rowley, E. Balzi, and A. Goffeau. 1995. Identification and characterization of SNQ2, a new multidrug ATP binding cassette transporter of the yeast plasma membrane. *J. Biol. Chem.* **270**:18150–18157.
- Decottignies, A., M. Kolaczowski, E. Balzi, and A. Goffeau. 1994. Solubilization and characterization of the overexpressed PDR5 multidrug resistance nucleotide triphosphatase of yeast. *J. Biol. Chem.* **269**:12797–12803.
- Delaveau, T., A. Delahodde, E. Carvajal, J. Subik, and C. Jacq. 1994. PDR3, a new yeast regulatory gene, is homologous to PDR1 and controls the multidrug resistance phenomenon. *Mol. Gen. Genet.* **244**:501–511.
- Dey, S., P. Hafkemeyer, I. Pastan, and M. M. Gottesman. 1999. A single amino acid residue contributes to distinct mechanisms of inhibition of the human multidrug transporter by stereoisomers of the dopamine receptor antagonist flupentixol. *Biochemistry* **38**:6630–6639.
- Dufour, J. P., A. Amory, and A. Goffeau. 1988. Plasma membrane ATPase from the yeast *Schizosaccharomyces pombe*. *Methods Enzymol.* **157**:513–528.
- Eliopoulos, G. M., and R. C. Moellering. 1991. Antimicrobial combinations, p. 432–492. In V. Lorian (ed.), *Antibiotics in laboratory medicine*, 3rd ed. The Williams and Wilkins Co., Baltimore, MD.
- Figler, R. A., H. Omote, R. K. Nakamoto, and M. K. Al-Shawi. 2000. Use of chemical chaperones in the yeast *Saccharomyces cerevisiae* to enhance heterologous membrane protein expression: high-yield expression and purification of human P-glycoprotein. *Arch. Biochem. Biophys.* **376**:34–46.
- Ford, J. M., and W. N. Hait. 1990. Pharmacology of drugs that alter multidrug resistance in cancer. *Pharmacol. Rev.* **42**:155–190.
- Gerberick, G. F., and P. A. Castric. 1980. In vitro susceptibility of *Pseudomonas aeruginosa* to carbenicillin, glycine, and ethylenediaminetetraacetic acid combinations. *Antimicrob. Agents Chemother.* **17**:732–735.
- Gietz, R. D., R. H. Schiestl, A. R. Willems, and R. A. Woods. 1995. Studies on the transformation of intact yeast cells by the LiAc/SS-DNA/PEG procedure. *Yeast* **11**:355–360.
- Goldstein, A. L., X. Pan, and J. H. McCusker. 1999. Heterologous URA3MX cassettes for gene replacement in *Saccharomyces cerevisiae*. *Yeast* **15**:507–511.
- Guarente, L. 1983. Yeast promoter and lacZ fusions designed to study expression of cloned genes in yeast. *Methods Enzymol.* **101**:181–191.
- Hendrich, A. B., O. Wesolowska, A. Pola, N. Motohashi, J. Molnar, and K. Michalak. 2003. Neither lipophilicity nor membrane-perturbing potency of phenothiazine maleates correlate with the ability to inhibit P-glycoprotein transport activity. *Mol. Membr. Biol.* **20**:53–60.
- Homolya, L., Z. Hollo, U. A. Germann, I. Pastan, M. M. Gottesman, and B. Sarkadi. 1993. Fluorescent cellular indicators are extruded by the multidrug resistance protein. *J. Biol. Chem.* **268**:21493–21496.
- Kaatz, G. W., V. V. Moudgal, S. M. Seo, and J. E. Kristiansen. 2003. Phenothiazines and thioxanthenes inhibit multidrug efflux pump activity in *Staphylococcus aureus*. *Antimicrob. Agents Chemother.* **47**:719–726.
- Katzmann, D. J., E. A. Epping, and W. S. Moye-Rowley. 1999. Mutational disruption of plasma membrane trafficking of *Saccharomyces cerevisiae* Yor1p, a homologue of mammalian multidrug resistance protein. *Mol. Cell. Biol.* **19**:2998–3009.
- Katzmann, D. J., P. E. Burnett, J. Golin, Y. Mahé, and W. S. Moye-Rowley. 1994. Transcriptional control of the yeast PDR5 gene by the PDR3 gene product. *Mol. Cell. Biol.* **14**:4653–4661.
- Kessel, D., W. T. Beck, D. Kukuruga, and V. Schulz. 1991. Characterization of multidrug resistance by fluorescent dyes. *Cancer Res.* **51**:4665–4670.
- Kolaczowska, A., M. Kolaczowski, A. Goffeau, and W. S. Moye-Rowley. 2008. Compensatory activation of the multidrug transporters Pdr5p, Snq2p, and Yor1p by Pdr1p in *Saccharomyces cerevisiae*. *FEBS Lett.* **582**:977–983.
- Kolaczowski, M., A. Kolaczowska, J. Luczynski, S. Witek, and A. Goffeau. 1998. In vivo characterization of the drug resistance profile of the major ABC transporters and other components of the yeast pleiotropic drug resistance network. *Microb. Drug Resist.* **4**:143–158.
- Kolaczowski, M., K. Michalak, and N. Motohashi. 2003. Phenothiazines as potent modulators of yeast multidrug resistance. *Int. J. Antimicrob. Agents* **22**:279–283.
- Kolaczowski, M., M. van der Rest, A. Cybularz-Kolaczowska, J. P. Soumillion, W. N. Konings, and A. Goffeau. 1996. Anticancer drugs, ionophoric peptides, and steroids as substrates of the yeast multidrug transporter Pdr5p. *J. Biol. Chem.* **271**:31543–31548.
- Laemmli, U. K. 1970. Cleavage of structural proteins during the assembly of the head of bacteriophage T4. *Nature* **227**:680–685.
- Leppert, G., R. McDevitt, S. C. Falco, T. K. Van Dyk, M. B. Ficke, and J. Golin. 1990. Cloning by gene amplification of two loci conferring multiple drug resistance in *Saccharomyces*. *Genetics* **125**:13–20.
- Liu, R., A. Siemiarz, and F. J. Sharom. 2000. Intrinsic fluorescence of the

- P-glycoprotein multidrug transporter: sensitivity of tryptophan residues to binding of drugs and nucleotides. *Biochemistry* **39**:14927–14938.
31. Longtine, M. S., A. McKenzie III, D. J. Demarini, N. G. Shah, A. Wach, A. Brachat, P. Philippsen, and J. R. Pringle. 1998. Additional modules for versatile and economical PCR-based gene deletion and modification in *Saccharomyces cerevisiae*. *Yeast* **14**:953–961.
  32. Mahé, Y., Y. Lemoine, and K. Kuchler. 1996. The ATP binding cassette transporters Pdr5 and Snq2 of *Saccharomyces cerevisiae* can mediate transport of steroids in vivo. *J. Biol. Chem.* **271**:25167–25172.
  33. Marchetti, O., P. Moreillon, M. P. Glauser, J. Bille, and D. Sanglard. 2000. Potent synergism of the combination of fluconazole and cyclosporine in *Candida albicans*. *Antimicrob. Agents Chemother.* **44**:2373–2381.
  34. Markham, P. N., E. Westhaus, K. Klyachko, M. E. Johnson, and A. A. Neyfakh. 1999. Multiple novel inhibitors of the NorA multidrug transporter of *Staphylococcus aureus*. *Antimicrob. Agents Chemother.* **43**:2404–2408.
  35. Motohashi, N., M. Kawase, J. Molnár, L. Ferenczy, O. Wesolowska, A. B. Hendrich, M. Bobrowska-Hägerstrand, H. Hägerstrand, and K. Michalak. 2003. Antimicrobial activity of *N*-acylphenothiazines and their influence on lipid model membranes and erythrocyte membranes. *Arzneimittelforschung* **53**:590–599.
  36. Munder, T., and A. Hinnen. 1999. Yeast cells as tools for target oriented screening. *Appl. Microbiol. Biotechnol.* **52**:311–320.
  37. Nakamura, K., M. Niimi, K. Niimi, A. R. Holmes, J. E. Yates, A. Decottignies, B. C. Monk, A. Goffeau, and R. D. Cannon. 2001. Functional expression of *Candida albicans* drug efflux pump Cdr1p in a *Saccharomyces cerevisiae* strain deficient in membrane transporters. *Antimicrob. Agents Chemother.* **45**:3366–3374.
  38. National Committee for Clinical Laboratory Standards. 1997. Reference method for broth dilution antifungal susceptibility testing of yeasts. Approved standard M27-A. National Committee for Clinical Laboratory Standards, Wayne, PA.
  39. Niimi, K., D. R. Harding, R. Parshot, A. King, D. J. Lun, A. Decottignies, M. Niimi, S. Lin, R. D. Cannon, A. Goffeau, and B. C. Monk. 2004. Chemosensitization of fluconazole resistance in *Saccharomyces cerevisiae* and pathogenic fungi by a D-octapeptide derivative. *Antimicrob. Agents Chemother.* **48**:1256–1271.
  40. Odds, F. C. 2003. Synergy, antagonism, and what the checkerboard puts between them. *J. Antimicrob. Chemother.* **52**:1.
  41. Pfaller, M. A., and D. J. Diekema. 2002. Role of sentinel surveillance of candidemia: trends in species distribution and antifungal susceptibility. *J. Clin. Microbiol.* **40**:3551–3557.
  42. Prasad, R., N. A. Gaur, M. Gaur, and S. S. Komath. 2006. Efflux pumps in drug resistance of *Candida*. *Infect. Disord. Drug Targets* **6**:69–83.
  43. Prasad, R., P. De Wergifosse, A. Goffeau, and E. Balzi. 1995. Molecular cloning and characterization of a novel gene of *Candida albicans*, CDR1, conferring multiple resistance to drugs and antifungals. *Curr. Genet.* **4**:320–329.
  44. Ramu, A., and N. Ramu. 1992. Reversal of multidrug resistance by phenothiazines and structurally related compounds. *Cancer Chemother. Pharmacol.* **30**:165–173.
  45. Reid, R. J. D., M. Lisby, and R. Rothstein. 2002. Cloning-free genome alterations in *Saccharomyces cerevisiae* using adaptamer-mediated PCR. *Methods Enzymol.* **350**:258–277.
  46. Sanglard, D., and J. Bille. 2002. Current understanding of the modes of action and resistance mechanisms to conventional and emerging antifungal agents for treatment of *Candida* infections, p. 349–387. In R. A. Calderone (ed.), *Candida and candidiasis*. ASM Press, Washington, DC.
  47. Sanglard, D., F. Ischer, M. Monod, and J. Bille. 1996. Susceptibilities of *Candida albicans* multidrug transporter mutants to various antifungal agents and other metabolic inhibitors. *Antimicrob. Agents Chemother.* **40**:2300–2305.
  48. Sanglard, D., F. Ischer, M. Monod, and J. Bille. 1997. Cloning of *Candida albicans* genes conferring resistance to azole antifungal agents: characterization of *CDR2*, a new multidrug ABC transporter gene. *Microbiology* **143**:405–416.
  49. Sarkadi, B., L. Homolya, and Z. Hollo. August 2001. Assay and reagent kit for evaluation of multi-drug resistance in cells. U.S. patent 6,277,655.
  50. Servos, J., E. Haase, and M. Brendel. 1993. Gene *SNQ2* of *Saccharomyces cerevisiae*, which confers resistance to 4-nitroquinoline-*N*-oxide and other chemicals, encodes a 169 kDa protein homologous to ATP-dependent permeases. *Mol. Gen. Genet.* **236**:214–218.
  51. Shukla, S., P. Saini, Smriti, S. Jha, S. V. Ambudkar, and R. Prasad. 2003. Functional characterization of *Candida albicans* ABC transporter Cdr1p. *Eukaryot. Cell* **2**:1361–1375.
  52. Sikorski, R. S., and P. Hieter. 1989. A system of shuttle vectors and yeast host strains designed for efficient manipulation of DNA in *Saccharomyces cerevisiae*. *Genetics* **122**:19–27.
  53. Souid, A. K., C. Gao, L. Wang, E. Milgrom, and W. C. Shen. 2006. *ELMI* is required for multidrug resistance in *Saccharomyces cerevisiae*. *Genetics* **173**:1919–1937.
  54. Tanabe, K., E. Lamping, K. Adachi, Y. Takano, K. Kawabata, Y. Shizuri, M. Niimi, and Y. Uehara. 2007. Inhibition of fungal ABC transporters by unnarmicin A and unnarmicin C, novel cyclic peptides from marine bacterium. *Biochem. Biophys. Res. Commun.* **364**:990–995.
  55. Torelli, R., B. Posteraro, S. Ferrari, M. La Sorda, G. Fadda, D. Sanglard, and M. Sanguinetti. 2008. The ATP-binding cassette transporter-encoding gene *CgSNQ2* is contributing to the *CgPDR1*-dependent azole resistance of *Candida glabrata*. *Mol. Microbiol.* **68**:186–201.
  56. Towbin, H., T. Staehelin, and J. Gordon. 1979. Electrophoretic transfer of proteins from polyacrylamide gels to nitrocellulose sheets: procedure and some applications. *Proc. Natl. Acad. Sci. USA* **76**:4350–4354.
  57. Weiss, J., S. M. Dormann, M. Martin-Facklam, C. J. Kerpen, N. Ketabi-Kiyanvash, and W. E. Haefeli. 2003. Inhibition of P-glycoprotein by newer antidepressants. *J. Pharmacol. Exp. Ther.* **305**:197–204.
  58. White, R. L., D. S. Burgess, M. Manduru, and J. A. Bosso. 1996. Comparison of three different in vitro methods of detecting synergy: time-kill, checkerboard, and E test. *Antimicrob. Agents Chemother.* **40**:1914–1918.
  59. White, T. C., S. Holleman, F. Dy, L. F. Mirels, and D. A. Stevens. 2002. Resistance mechanisms in clinical isolates of *Candida albicans*. *Antimicrob. Agents Chemother.* **6**:1704–1713.
  60. Wilson, R. B., D. Davis, B. M. Enloe, and A. P. Mitchell. 2000. A recyclable *Candida albicans* *URA3* cassette for PCR product-directed gene disruptions. *Yeast* **16**:65–70.
  61. Yang, H. C., Y. Mikami, T. Imai, H. Taguchi, K. Nishimura, M. Miyaji, and M. L. Branchini. 2001. Extrusion of fluorescein diacetate by multidrug-resistant *Candida*. *Mycoses* **44**:368–374.
  62. Zhang, J. H., T. D. Y. Chung, and K. R. Oldenburg. 1999. A simple statistical parameter for use in evaluation and validation of high throughput screening assays. *J. Biomol. Screen.* **4**:67–73.